

Power Laws, Precursors and Predictability During Failure

RUMI DE¹(*) and G. ANANTHAKRISHNA^{1,2}(**)

¹ *Material Research Center, Indian Institute of Science, Bangalore-560012, India.*

² *Center for Condensed Matter Theory, Indian Institute of Science, Bangalore-560012, India.*

PACS. 74.25.Ld – Mechanical and acoustical properties, elasticity and ultrasonic attenuation.

PACS. 91.30.Px – Phenomena related to earthquake prediction.

PACS. 64.60.Ht – Dynamic critical phenomena.

Abstract. – We investigate the dynamics of a modified Burridge-Knopoff model by introducing a dissipative term to mimic the bursts of acoustic emission (AE) from rock samples. The model explains many features of the statistics of AE signals observed in experiments such as the crossover in the exponent value from relatively small amplitude AE signals to larger regime, and their dependence on the pulling speed. Significantly, we find that the cumulative energy dissipated identified with acoustic emission can be used to predict a major slip event. We also find a data collapse of the acoustic activity for several major slip events describable by a universal stretched exponential with corrections in terms of time-to-failure.

Predicting failure of materials is of interest in science and engineering (electrical breakdown, fracture of laboratory samples to engineering structures) particularly so in seismology due to the enormous damage earthquakes can cause. Whether it is at a laboratory or geological scale, this amounts to identifying useful precursors at a statistically significant level. One important non-destructive tool in fracture studies is the acoustic emission (AE) technique as it is sensitive to the microstructural changes occurring in the sample. Insight into earthquake dynamics has been obtained through fracture studies of (usually pre-cut samples to mimic slip on preexisting tectonic faults) rock samples [1]. Such studies have established that there is a considerable overlap between AE and seismology as both are concerned about the generation and propagation of elastic waves. Quite early, the statistics of the AE signals was shown to exhibit a power law [1–3] similar to the Gutenberg-Richters law for the magnitudes of earthquakes [4] and Omori's law for aftershocks [2, 5]. These prompted further investigations to look for precursor effects that can be used for earthquake predictability [5–8].

Apart from the power law distributions observed in the AE signals during fracture, acoustic activity of unusually large number of situations as varied as volcanic activity [9], micro-fracturing process [10,11], and collective dislocation motion [12], exhibits power laws statistics. Though the general mechanism attributed to AE is the release of stored strain energy, the details are system specific. Thus, the ubiquity of the power law statistics of AE signals suggests that the details of the underlying processes are irrelevant. Indeed, the conceptual

(*) E-mail: rumi@mrc.iisc.ernet.in

(**) E-mail: garani@mrc.iisc.ernet.in

framework of self-organized criticality (SOC) was introduced to explain the universality of power law statistics in varied systems [13, 14]. This brings up a related *puzzle* that lack of intrinsic length scales and time scales in power law systems has been taken to mean *lack of predictability of individual avalanches* [5, 15]. This generally held opinion has also triggered considerable debate regarding earthquake predictability, as seismically active fault systems are considered to be in a SOC state [15]. Thus, it would be desirable to design a model which exhibits power law statistics where predictability of individual events is possible.

On the other hand, there has been reports of increased levels of AE signals before failure of rock samples [6, 16, 17], in experiments on laboratory samples [18, 19] and precursory effects in individual earthquakes as well [5, 7, 20, 21]. There has been attempts to predict failure within the framework of time-to-failure (TTF) models, both on the laboratory level [18] as well on geological scale [22]. (Some efforts have also been made on the predictability of avalanches in SOC state [23].) However, as the primary aim of TTF models is to mimic the rate of increase in precursory variable, they are independent of the nature of the variable. Thus, if one is interested explaining the origin of increasing level of activity in AE signals observed in experiments as the system approaches failure, it is necessary to first model AE in terms of displacement related variable as AE corresponds to high frequency elastic waves. Here, we model AE signals by introducing an additional dissipative term into Burridge-Knopoff model [24–26] that helps us to identify precursory effect and hence to predict slip events.

Our second objective is to explain some recent results on AE studies on rock samples. These studies report an interesting crossover in the exponent value from small amplitude regime to large [28], a result that is similar to the well noted observation on the change in the power law exponent for small and large magnitudes earthquakes [29]. The exponent value is also found to be sensitive to the deformation rate [30]. To the best of our knowledge, *there has been no explanation of these observations*. This can partly be traced to the lack of efforts to model AE signals in terms of *displacement related variables*.

Deformation and/or breaking of the asperities results in an accelerated motion of the local areas of slip where the stored potential energy is converted to kinetic energy. The general mechanism attributed to acoustic emission is the sudden release of the stored strain energy. In the case of modeling AE signals involving abrupt dislocation motion, the energy of AE signals, $E_{ae}(r)$ is taken to be proportional $\dot{\epsilon}^2(r)$, where $\dot{\epsilon}$ is the local plastic strain rate [31]. However, in general there is spatial inhomogeneity which implies that total energy $E_{ae} \propto \int (\nabla \dot{\epsilon})^2 d^3r$. For the BK model, displacement rate takes the role of $\dot{\epsilon}$. On the other hand, E_{ae} , has the same form as the Rayleigh dissipation functional [32] arising from the rapid movement of a localized region. Such a rapid movement prevents the system from attaining a quasi-static equilibrium which in turn generates dissipative forces that resist the rapid motion. On general grounds this dissipative forces has been shown to be proportional to $\int (\nabla v)^2 d^3r$, where v is the local velocity. Such a term is termed as solid viscosity in parallel with shear viscosity of fluids. (We ignore other types of dissipation such as radiation damping.) Indeed, we have found that the above term mimics all the features of the AE signals observed during martensitic transformation [33] (both the power law statistics of the AE signals during thermal cycling and the highly correlated AE signals associated with growth and shrinkage of martensite domains).

The Burridge-Knopoff (BK) model for earthquakes [24] and its variants are popular models among the physics community. Despite its limitation (lack of appropriate continuum limit) [26, 27], it forms a convenient platform to investigate the question of predictability of large avalanches as the dissipated energy bursts (in our modified model) themselves follow a power law distribution. The model consists of a chain of blocks of mass m coupled to each other by coil springs of strength k_c and attached to a fixed surface by leaf springs of strength k_p as

shown in Fig. 1. The blocks are in contact with a rough surface moving at constant speed v (mimicking the points of contact between two tectonic plates). A crucial input into the model is the velocity-dependent frictional force between the blocks and the surface (see Fig. 1).

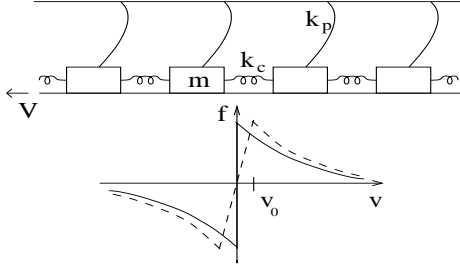


Fig. 1

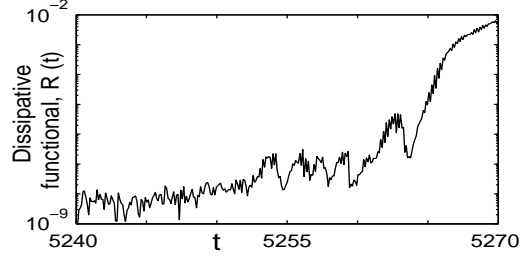


Fig. 2

Fig. 1 – The Burridge-Knopoff spring block model and the two forms of friction laws used.

Fig. 2 – Dissipative functional, $R(t)$ as a function of t .

The additional dissipative force is introduced through the Lagrange's equations of motion given by $\frac{d}{dt} \left(\frac{\delta L}{\delta \dot{u}(x)} \right) - \frac{\delta L}{\delta u(x)} = - \frac{\delta F}{\delta \dot{u}(x)}$ with the Lagrangian $L = T - P$. The kinetic energy T is defined by $T = \frac{m}{2} \int \left(\frac{\partial u(x)}{\partial t} \right)^2 dx$, and the potential energy by $P = \frac{1}{2} \int [k_c \left(\frac{\partial u(x)}{\partial x} \right)^2 + k_p (u(x))^2] dx$. Here u is the displacement of the blocks measured from the initial equilibrium position. The Rayleigh dissipative functional [32] is given by $R = \frac{\gamma}{2} \int \left(\frac{\partial \dot{u}(x)}{\partial x} \right)^2 dx$, where γ is a dissipation coefficient. The total dissipation F is the sum of $R(t)$ and frictional dissipation given by $F_{fr} = \int [f(v + \dot{u}(x))] dx$, where the over dot refers to the time derivative and the frictional force is taken to be derivable from a potential like function. Then the equation of motion is

$$m \frac{\partial^2 u}{\partial t^2} = k_c \frac{\partial^2 u}{\partial x^2} - k_p u - \frac{\partial f(\dot{u} + v)}{\partial \dot{u}} + \gamma \frac{\partial^2 \dot{u}}{\partial x^2}, \quad (1)$$

The discretized version, in the notation of Ref [25], reads

$$\ddot{U}_j = l^2 (U_{j+1} - 2U_j + U_{j-1}) - U_j - \phi(2\alpha\nu + 2\alpha\dot{U}_j) + \gamma_c (\dot{U}_{j+1} - 2\dot{U}_j + \dot{U}_{j-1}), \quad (2)$$

where U_j is the dimensionless displacement of the j^{th} block, ν the dimensionless pulling velocity, $l^2 = k_c/k_p$ the ratio of the slipping time to the loading time, and α is the rate of velocity-weakening in the scaled frictional force ϕ (see Fig. 1). The Coulomb frictional law is shown by the solid line. The dashed curve uses a resistive creep branch ending at v_0 ($\sim 10^{-7}$ here) beyond which the velocity weakening law operates. γ_c is the scaled dissipation coefficient. The continuum limit of Eq. (2) exists for the creep branch (even in the absence of $R(t)$) which ensures a length scale below which all perturbations are damped [25]. Such a length scale is absent for the Coulomb case even as the continuum limit exists due to the additional dissipative term. These differences between the frictional laws may influence the nature of the statistics which we investigate in detail.

This model without the last term has been extensively studied [24–26]. Starting from random initial conditions for all the blocks, slip events ranging from one-block event to those extending over the entire fault (occurring roughly once in a loading period $\tau_L \sim 2/\nu$) are seen in the steady state for both types of frictional laws.

Equation (2) has been solved using a fourth-order Runge-Kutta method with open boundary condition for both types of frictional laws shown in Fig. 1. Random initial conditions are

imposed. After discarding the initial transients, long data sets are recorded when the system has reached a stationary state. The parameters used here are $l = 10, \alpha = 2.5, N = 100, 200$ for $\nu = 0.01$ and 0.001 and a range of values of γ_c . The modified BK model produces the same statistics of slip events as that without the last term in Eq. (2) as long as the value of γ_c is small, typically $\gamma_c < 0.5$. The results presented here are for $N = 100$ and $\gamma_c = 0.02$.

Since the rate of energy dissipated [32] due to local accelerating blocks is given by $dE_{ae}/dt = -2R(t)$, we calculate $R(t)$ which exhibits bursts similar to the AE signals observed in experiments. A plot of $R(t)$ for the case with Coulomb frictional law is shown in Fig. 2. For the case with creep branch, $R(t)$ is less noisy.

We now consider the statistics of the energy bursts $R(t)$. Denoting A to be the amplitude of $R(t)$ (*i.e.*, from a maximum to the next minimum), we find that the distribution of the magnitudes $D(A)$ (accumulated over 2×10^5 time steps), shows a power law $D(A) \sim A^{-m}$. Instead of a single power law anticipated, we find that the distribution shows two regions, one for relatively smaller amplitudes and another for large values shown by the two distinct plots for the Coulomb case shown in Fig. 3. (The crossover in the power law exponent from smaller to larger amplitude region is seen as a scatter at the upper end of $A \sim 10^{-5}$.) Similar results are obtained when the frictional law has a creep branch. The value of m for the small amplitudes region (typically $< 10^{-4}$) is $\sim 1.78 \pm 0.01$, significantly smaller than that for large amplitudes which is $\sim 2.09 \pm 0.02$, consistent with the recent experimental result on AE of rock samples [28]. The increase in the exponent value mimics a similar observation for large magnitude earthquakes (> 7.0 on the Richter scale [29]).

Recently Yabe *et al.* [30] have reported that the exponent value corresponding to relatively small amplitude regime increases with decreasing deformation rate while that for the large amplitude regime is found to be insensitive. To check this, we have calculated $D(A)$ for $\nu = 0.001$ shown in Fig. 3 which shows that the exponent for small amplitude increases to 1.91 ± 0.02 . However, we find that the exponent for larger amplitude regime is insensitive (not shown) to the changes in ν .

This result can be physically explained by analyzing the influence of the pulling velocity on slip events of varying sizes. We first note that $R(t)$ depends on the difference in the velocities of neighboring blocks. The velocity of ‘microscopic’ events (small number of blocks) has been shown to be proportional to ν [25]. For single block events, as the neighboring blocks are at rest, the number of such events are fewer in proportion to the pulling speed, both of which are evident from Fig. 3. For the two block events, the contribution comes mostly from the edges as the difference in the velocities of the two blocks are of similar magnitude. In a similar way, it can be argued that for slip events of finite size, the extent of the contribution to $R(t)$ is decided by the ruggedness of the velocity profile within the slipping region; the magnitude of $R(t)$ is lower if the velocity is smoother. The ruggedness of the velocity profile, however, is itself decided by how much time the system gets to ‘relax’. At lower values of ν , there is sufficient time for the blocks to attain nearly the same velocities as the neighboring blocks compared to that at higher ν values. Thus, the larger slip events contribute lesser to $R(t)$ for smaller ν values and hence the slope of $\log D(A)$ increases for smaller value of ν .

Now we consider the possibility of a precursor effect. A plot of $R(t)$ is shown in the inset of Fig. 4 for the frictional law with a creep branch. *A gradual increase in the activity of the energy dissipated can be seen which accelerates just prior to the occurrence of a ‘major’ slip event.* The rapid increase in $R(t)$ coincides with the abrupt increase in the mean kinetic energy (KE). Here, we have used KE as a measure of event size as it is a good indicator of the magnitude of the slip events. We find similar increase in $R(t)$ for all ‘major’ slip events. (In our simulations, the KE of observable events ranges from 10^{-4} to 0.2 . We refer to all such events as ‘major’ events.) This suggests that $R(t)$ can be used as a precursor for the onset of a

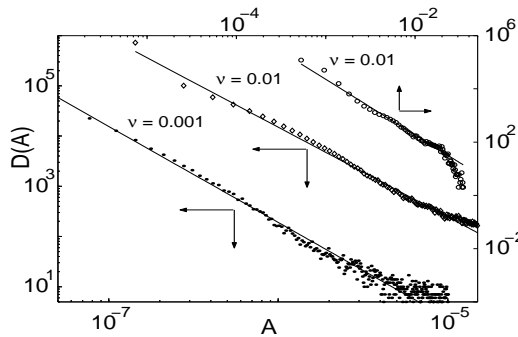


Fig. 3

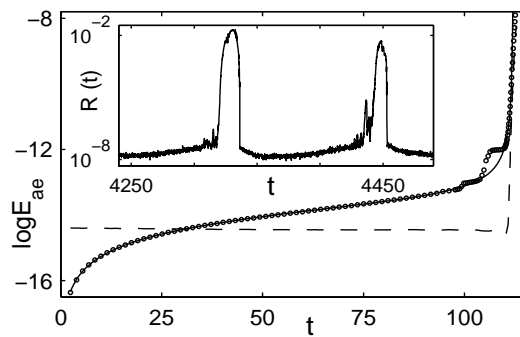


Fig. 4

Fig. 3 – Distribution of amplitudes of $R(A)$, $D(A)$ versus A . for small amplitudes (\diamond for $\nu = 0.01$ \bullet for $\nu = 0.001$) and large amplitudes (\circ for $\nu = 0.01$ shifted up for clarity).

Fig. 4 – A semi-log plot of the cumulative energy, E_{ae} versus t (\circ) along with the fit (solid line). Dashed line corresponds to the mean kinetic energy. The inset shows $R(t)$ as a function of t .

major slip event. As $R(t)$ is noisy, a better quantity for the analysis is the cumulative energy dissipated $E_{ae}(t)$ ($\propto \int_0^t R(t')dt'$). $E_{ae}(t)$ grows in a stepped manner with their magnitudes increasing as we approach a major event. A plot of $\log E_{ae}$ is shown in Fig. 4 along with a fit (continuous curve) having the functional form,

$$\log E_{ae}(t) = -a_1 t^{-\alpha_1} [1 - a_2 |(t - t_c)/t_c|^{-\alpha_2}]. \quad (3)$$

Here, t is the time measured from some initial point after a major event. The constants a_1, a_2, α_1 and α_2 and t_c are adjustable. The crucial parameter t_c is the time of occurrence of a major slip event (often referred to as the ‘failure’ point). It is clear that the fit is striking. Given a reasonable stretch of the data, the initial increasing trend in $\log E_{ae}$ is easily fitted to a stretched exponential, *i.e.*, $-a_1 t^{-\alpha_1}$. The additional term is introduced to account for the observed rapid increase in the activity as we approach the major event. In contrast, the mean kinetic energy increases abruptly on reaching the event (dashed line). It is clear that the estimated t_c agrees quite well with that of KE of the event.

Now, we address the question of predictability of major slip events using $E_{ae}(t)$. This is equivalent to determining the correct t_c . Given $E_{ae}(t)$ over a reasonable initial stretch of time, say till t_1 (the first arrow in Fig. 5), we find that the four constants a_1, a_2, α_1 and α_2 are already well determined (within a small error bar). These change very little with time. (Only t_c changes.) A fit to Eq. (3) also gives $t_c^{(1)}$ at t_1 (which can only be considered as an estimate based on the data till t_1). One such curve is shown by a dashed line with the arrow shown at t_1 . However, as time progresses, the data accumulated later usually deviates from the predicted curve if t_c is inaccurate as is the case for the fits till t_1 and t_2 for instance (Fig. 5). If on the other hand, the deviation of the predicted curve from the accumulated data decreases with passage of time within the error bar (as is the case for the region just before t_3), then, the value of t_c is likely to be accurate. Indeed, the extrapolated continuous curve corresponding to data fit till $t = t_3$ (third arrow in Fig. 5) with the predicted $t_c^{(3)}$ is seen to follow the data very well. (Usually, the data deviates from the predicted curve with a sudden decrease in E_{ae}^{-1} which is again an indication of a coherent slipping of several blocks before the onset of a fully delocalized event. But the general trend soon follows the extrapolated curve.)

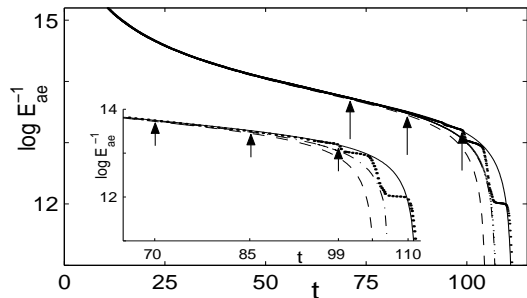


Fig. 5

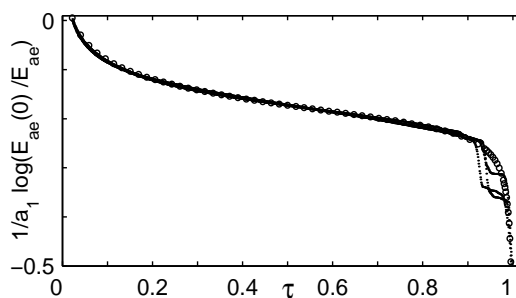


Fig. 6

Fig. 5 – A plot of $\log E_{ae}^{-1}$ versus t . Inset shows the enlarged section at time t_1 (–), t_2 (–·) and t_3 (solid line). Data shown (·) is indistinguishable from the fit till t_3 .

Fig. 6 – Collapsed data using $a_1^{-1} \log(E_{ae}(0)/E_{ae}(\tau))$ vs. τ for three different events along with the fit shown by (o).

Then, t_3 can be taken as the warning time for the onset of the major event. The actual t_c read off from the kinetic energy plots is 111.0 where as the predicted t_c is 111.6 giving the accuracy in the prediction of correct t_c to be $\sim 99.5\%$. This fit is obtained when t_{last} is 12% away from the true t_c . Similar numbers are obtained for several other events fitted. If the approach to all slip events is described by the scale invariant form, then one should expect to find a data collapse for different events. Indeed, in terms of a scaled time $\tau = t/t_c$, we find that the data corresponding to different events collapses into a single curve given by

$$a_1^{-1} \log[E_{ae}(0)/E_{ae}(\tau)] = \tau^{-\alpha_1} [1 - a_2 |(\tau - 1)|^{-\alpha_2}] + a_1^{-1} \log E_{ae}(0). \quad (4)$$

A plot corresponding to three different events is shown in Fig. 6 along with the fit. The results are similar when the Coulomb frictional law is used except that $R(t)$ is more noisy and hence prone to slightly larger errors in predicted t_c .

In summary, the model captures several experimentally observed features of acoustic emission such as the two different exponent values in the power law statistics for small and large amplitude regimes with the former being more sensitive to the pulling speed. The dependence of the exponent on the pulling speed has been traced to the form of $R(t)$, namely, the gradient of the local velocity. More significantly, the analysis shows that it is possible to predict a major event fairly accurately. This result demonstrates that *power law statistics in itself does not preclude predictability* (of individual events). Further, we note that a SOC state demands that all observable quantities should follow a scale invariant form which is *clearly respected* by Eqs. (3,4) representing the approach to all events. The data collapse for different events into a scale free form clearly suggests that the dynamics of approach to major events is universal.

A few comments are in order. We stress that this precursor effect is absent in the total kinetic energy or seismic moments. As there is no correspondence between seismic moments or the KE of the events with $R(t)$ (which depends on the difference between the velocities of neighboring elements), our analysis cannot predict the magnitudes of the slip events. Indeed, in some cases we find that $R(t)$ is larger for a smaller slip event, as is the case for the two peaks in $R(t)$ shown in Fig. 4. We point out here that the gradual increase in the energy dissipated as we approach a major event is different from that reported in the context of the BK model [34]. Our work also differs from the approach of Huang *et al.* [22] in the sense that in their analysis, the hierarchical structure and long range interaction are necessary ingredients

for the power law approach to failure with log periodic corrections that arises due to discrete scale invariance [19, 22]. As far as we know, this is the first time that reproduces several unexplained experimental results on AE of rock samples [28, 30]. We believe that it would be possible to address the problem of predictability in other power situations, which however, may demand capturing the essential physics of the relevant precursor effect.

RD wishes to thank Dr. S. Rajesh and Dr. M. S. Bharathi for useful discussions. This work is supported by Department of Science and Technology, Grant No. Sp/s2K-26/98, New Delhi, India.

REFERENCES

- [1] LOCKNER A. *et al.*, *Nature*, **350** (1991) 39; LOCKNER A., *Int. J. Rock Mech. Min. Sci. and Geomech. Abstr.*, **30** (1993) 883.
- [2] MOGI K., *Bull. Earthquake Res. Inst.*, **40** (1962) 125.
- [3] SCHOLZ C. H., *Bull. Seismol. Soc. Am.*, **58** (1968) 399.
- [4] GUTENBERG. B. and RICHTER C. F., *Ann. Geofis.*, **9** (1596) 1.
- [5] MAIN I., *Rev. Geophys.*, **34** (1996) 433.
- [6] SAMMONDS P. R., MEREDITH P. G. and MAIN I. G., *Nature*, **359** (1992) 282.
- [7] MAIN I. G. AND MEREDITH P. G., *Tectonophysics*, **167** (1989) 273.
- [8] HAINZL S., ZOLLER G. AND KURTHS J., *Geophys. Res. Lett.*, **27** (2000) 597.
- [9] DIODATI P., MARCHESONI F. and PIAZZA S., *Phys. Rev. Lett.*, **67** (1991) 2239.
- [10] PETRI A. *et al.*, *Phys. Rev. Lett.*, **73** (1994) 3423.
- [11] TZSCHICHHOLZ F. and HERRMANN H. J., *Phys Rev. E*, **51** (1995) 1961.
- [12] C. MIGUEL M. *et al.*, *Nature*, **410** (2001) 667.
- [13] BAK P., TANG C. and WIESENFELD K., *Phys. Rev. Lett.*, **59** (1987) 381.
- [14] JENSEN H. J., *Self-Organised Criticality* (Cambridge University Press, Cambridge) 1998.
- [15] *Nature debate*, (1999) . Is the reliable prediction of individual earthquakes a realistic scientific goal? <http://helix.nature.com/debates/earthquake>.
- [16] SCHOLZ C. H., *J. Geophys. Res.*, **73** (1968) 1417.
- [17] LOCKNER A., *J. Acous. Emission*, **14** (1996) S88.
- [18] GUARINO A. *et al.*, *Eur. Phys. J. B*, **26** (2002) 141 and the references therein.
- [19] JOHANSEN A. and SORNETTE D., *Eur.Phys.B.*, **18** (2000) 163.
- [20] SYKES L. R. AND JAUM S., *Nature*, **348** (1990) 595.
- [21] BUFE C. G. AND VARNES D. J., *J. Geophys. Res.*, **98** (1990) 9871.
- [22] HUANG Y., SALEUR H., SAMMIS C. and SORNETTE D., *Europhys. Lett.*, **41** (1998) 43; HUANG Y., SALEUR H. and SORNETTE D., *J. Geophys. Res.*, **105** (2000) 28111.
- [23] ROSENDAHL J., VEKIC M. and RUTLEDGE J. E., *Phys. Rev. Lett.*, **73** (1994) 537; ACHARYYA M. and CHAKRABARTI B. K., *Phys. Rev. E*, **53** (1996) 140. PEPKE S. L. AND CARLSON J. M., *Phys. Rev. E*, **50** (1994) 236.
- [24] BURRIDGE R. and KNOPOFF L., *Bull. Seismol. Soc. Am.*, **57** (1967) 341.
- [25] CARLSON J. M., AND LANGER J. S., *Phys. Rev. Lett.*, **62** (1989) 2632; *Phys. Rev. A*, **40** (1989) 6470.
- [26] SCHMITTBUHL J., VILOTTE J. P. AND ROUX S., *Europhys.Lett.*, **21** (1993) 375. SCHMITTBUHL J., VILOTTE J. P. AND ROUX S., *J. Geophys. Res.*, **101**, **B12** (1996) 27714.
- [27] RICE J., *J. Geophys. Res.*, **98** (1993) 9885; RICE J. AND BEN-ZION, *Proc. Natl. Acad. Sci. USA*, **93** (1996) 3811.
- [28] YABE Y., KATO N., YAMAMOTO K. and HIRASAWA T., *Pure Appl. Geophys.*, **160** (2003) 1163
- [29] PACHECO J. F., SCHOLZ C. H. and SYKES L. R., *Nature*, **355** (1992) 71.
- [30] YABE Y., *Geophys. Res. Lett.*, **29** (2002) 10.1029/2001GL014369.
- [31] J. WEISS *et al.*, *J. Geo. Research*, **105** (2000) 433.
- [32] LANDAU L. D. and LIFSCHITZ E. M., *Theory of Elasticity* (Pergamon, Oxford) 1986.

- [33] AHLUWALIA R. and ANANTHAKRISHNA G., *Phys. Rev. Lett.*, **86** (2001) 4076; SREEKALA S. and ANANTHAKRISHNA, *Phys. Rev. Lett.*, **90** (135501) 2003.
- [34] SHAW B. E., CARLSON J. M. AND LANGER J. S., *J. Geophys. Res.*, **97** (1992) 479.